Journal of Industrial Microbiology & Biotechnology (2018) 45:681–696
https://doi.org/10.1007/s10295-018-2048-y

FERMENTATION, CELL CULTURE AND BIOENGINEERING - ORIGINAL PAPER

Metabolomic and proteomic analysis of D-lactate-producing *Lactobacillus delbrueckii* under various fermentation conditions

Shaoxiong Liang[1,2] · Dacheng Gao[3] · Huanhuan Liu[4,5] · Cheng Wang[1,2] · Jianping Wen[1,2]

Received: 23 January 2018 / Accepted: 19 May 2018 / Published online: 28 May 2018

Abstract

As an important feedstock monomer for the production of biodegradable stereo-complex poly-lactic acid polymer, D-lactate has attracted much attention. To improve D-lactate production by microorganisms such as *Lactobacillus delbrueckii*, various fermentation conditions were performed, such as the employment of anaerobic fermentation, the utilization of more suitable neutralizing agents, and exploitation of alternative nitrogen sources. The highest D-lactate titer could reach 133 g/L under the optimally combined fermentation condition, increased by 70.5% compared with the control. To decipher the potential mechanisms of D-lactate overproduction, the time-series response of intracellular metabolism to different fermentation conditions was investigated by GC–MS and LC–MS/MS-based metabolomic analysis. Then the metabolomic datasets were subjected to weighted correlation network analysis (WGCNA), and nine distinct metabolic modules and eight hub metabolites were identified to be specifically associated with D-lactate production. Moreover, a quantitative iTRAQ–LC–MS/MS proteomic approach was employed to further analyze the change of intracellular metabolism under the combined fermentation condition, identifying 97 up-regulated and 42 down-regulated proteins compared with the control. The in-depth analysis elucidated how the key factors exerted influence on D-lactate biosynthesis. The results revealed that glycolysis and pentose phosphate pathways, transport of glucose, amino acids and peptides, amino acid metabolism, peptide hydrolysis, synthesis of nucleotides and proteins, and cell division were all strengthened, while ATP consumption for exporting proton, cell damage, metabolic burden caused by stress response, and bypass of pyruvate were decreased under the combined condition. These might be the main reasons for significantly improved D-lactate production. These findings provide the first omics view of cell growth and D-lactate overproduction in *L. delbrueckii*, which can be a theoretical basis for further improving the production of D-lactate.

Keywords D-lactate · Fermentation condition · Metabolomics · Proteomics · *Lactobacillus delbrueckii*

Introduction

As an important and multifunctional organic acid, D-lactate (D-LA) has been widely used in pharmaceutical, chemical, and cosmetic industries [12]. Especially, highly optical pure D-LA is a feedstock monomer for the production of biodegradable stereo-complex poly-lactic acid (SC-PLA) polymer. SC-PLA has an increased thermal tolerance up to 230 °C [11], which allows for a wide variety of applications in agricultural and motor vehicle-associated plastics [15, 47].

The industrial production of D-LA with high optical purity is usually conducted with bacteria, such as *Lactobacillus*, *E. coli,* and *C. glutamicum* [24]. However, *E. coli* and

Electronic supplementary material The online version of this article (https://doi.org/10.1007/s10295-018-2048-y) contains supplementary material, which is available to authorized users.

✉ Jianping Wen
jpwen@tju.edu.cn

[1] Key Laboratory of Systems Bioengineering (Ministry of Education), Tianjin University, Tianjin 300072, People's Republic of China

[2] SynBio Research Platform, Collaborative Innovation Center of Chemical Science and Engineering (Tianjin), Tianjin 300072, People's Republic of China

[3] Dalian Research Institute of Petroleum and Petrochemicals, SINOPEC, Dalian 116000, People's Republic of China

[4] State Key Laboratory of Food Nutrition and Safety, Tianjin University of Science and Technology, Tianjin 300457, China

[5] Key Laboratory of Food Nutrition and Safety, Ministry of Education, Tianjin University of Science and Technology, Tianjin 300457, China

C. glutamicum produce unwanted organic acid by-products, which need further extensive genetic modification [24]. *Lactobacillus delbrueckii* is an excellent genus of homofermentative D-LA bacteria with higher optical purity (≥98%), fewer by-products, and higher substrate utilization. Meanwhile, *L. delbrueckii* prefers a higher growth and fermentation temperature [21], which could not only decrease the risk of contaminations and the cooling cost of large-scale fermentation [1], but also match the optimum temperatures of most enzymes used in the process of simultaneous saccharification and fermentation (SSF) [24].

However, many factors (i.e., medium composition, growth condition, pH, and operation mode) have shown significant influence on the D-LA yield and optical purity [21]. To improve D-LA production, several strategies have been applied, such as selection of suitable neutralizing agents to reduce the inhibition of lactate [35], fed-batch fermentation to relieve the substrate inhibition [46], and continuous fermentation to decrease the supply of sub-raw material [31]. In addition, several researchers have also attempted to exploit alternative substrates to reduce the D-LA production cost, such as peanut meal [54] and lignocellulosic waste [27]. Nevertheless, there are few reports on the molecular mechanisms of D-LA overproduction influenced by the fermentation strategies and alternative substrates.

As a powerful tool, metabolomics has been widely applied to depict the intracellular metabolic profiles associated with the apparent metabolic differences [6], identify the biomarkers [5], and rationally optimize the medium [52]. Besides the most common statistical approaches used in metabolomic data analysis, i.e., principal component analysis (PCA) and partial least squares discriminant analysis (PLS-DA), a new approach named weighted correlation network analysis (WGCNA) has been recently proposed to describe the correlation relationships between clusters of highly correlated genes, proteins, metabolites or modules, and external conditions or sample traits [40], and has been widely applied to metabolomic analysis [40, 45, 51, 56]. Moreover, as an effective, accurate, and highly admitted proteomic technique, isobaric tags for relative and absolute quantitation (iTRAQ) approach has become a powerful tool in quantitative proteomics, especially for detecting hydrophobic and low-abundance proteins in cells and organelles under various physiological or environmental conditions [13, 22], and has been widely used in microorganisms [29, 53].

In this study, the influences of various fermentation conditions on D-LA production were compared comprehensively, including the employment of anaerobic fermentation by continuously inletting N_2, the utilization of alternative neutralizing agents [$Ca(OH)_2$ or NaOH] to control pH, and the exploitation of alternative nitrogen source (i.e., peptone and yeast extract). By applying the above conditions, the highest D-LA production was achieved (up to 133 g/L). To reveal the potential mechanisms of D-LA overproduction, a systematic research strategy was carried out. Gas chromatography–mass spectrometry (GC–MS) and liquid chromatography–mass spectrometry/mass spectrometry (LC–MS/MS)-based metabolomic approaches were employed to determine the time-series responses of *L. delbrueckii* to all the above fermentation conditions, and a weighted correlation network analysis (WGCNA) was constructed to reveal metabolic modules and hub metabolites significantly associated with each condition. Then, a quantitative iTRAQ proteomic approach was performed to capture the differential protein expression profiles of *L. delbrueckii* under the combined condition and the control. This report represents the first comprehensive study on metabolomic and proteomic analysis of D-LA-producing *L. delbrueckii* and the results will be a guidance to further strengthen the D-LA production.

Materials and methods

Microorganism and cultivations

Lactobacillus delbrueckii S-NL31 used in this study was stocked in our laboratory. Seed medium: modified MRS medium (pH 5.8) consisted of 1 g/L Tween 80, 10 g/L beef extract, 10 g/L peptone, 5 g/L yeast extract, 2 g/L ammonium citrate dibasic, 2 g/L K_2HPO_4, 3 g/L sodium acetate, 0.2 g/L $MgSO_4$, and 0.1 g/L $MnSO_4$, 20 g/L glucose. The production medium was the same as modified MRS medium except for carbon source and nitrogen source as shown in Table 1. The detailed fermentation conditions could also be seen in Table 1. The seed was statically cultivated in 250-ml flask containing 100-ml seed medium at 42 °C for 12 h. The D-LA production was carried out in 7.5-L BioFlo 110 fermenter (New Brunswick Scientific, Edison, NJ, USA) with a 5 L working volume at 150 rpm for 48 h at 42 °C after inoculating 500-mL seed culture. Three biological replicates were used for each fermentation experiment.

Analytical methods

The biomass yield was determined by dry cell weight (DCW). The residual glucose in fermentation broth was quantified using SBA-40C biosensor analyzer (Institute of Biology, Shandong Academy of Sciences, China). The concentration and optical purity of D-LA was measured by HPLC (Agilent 1200, USA) equipped with a chiral column (150 mm × 4.6 mm, SUMICHIRAL OA-5000) at 254 nm [2].

Table 1 Fermentation conditions used for D-LA production in this study

	Fermentation conditions
Control	Modified MRS medium with 30 g/L beef extract as sole nitrogen source, 80 g/L glucose as initial carbon source, excess $CaCO_3$ (50 g/L) as neutralizing agent, no aeration. Feeding about 4.6 g/(L h) glucose to the medium from 18 to 30 h
N_2	The same as control except for inletting 0.2 L/min nitrogen to the medium, continuing 0.5 h after inoculation
PE–YE	The same as control except for replacing beef extract with the combination of 20 g/L peptone and 10 g/L yeast extract
$Ca(OH)_2$	The same as control except for using calcium hydroxide as neutralizing agent, and automatically adjusting pH between 5.9 and 6.0
NaOH	The same as control except for using sodium hydroxide as neutralizing agent, and automatically adjusting pH between 5.9 and 6.0.
N_2–PE–YE–$Ca(OH)_2$	Optimally combined fermentation conditions, i.e., modified MRS medium with 20 g/L peptone and 10 g/L yeast extract as nitrogen source, 80 g/L glucose as initial carbon source, calcium hydroxide as neutralizing agent, and automatically adjusting pH between 5.9 and 6.0. Inletting 0.2 L/min nitrogen to the medium, continuing 0.5 h after inoculation. Feeding about 4.6 g/(L h) glucose to the medium from 18 to 30 h

GC–MS and LC–MS/MS-based metabolomic analysis

To analyze the intracellular metabolic responses of *L. delbrueckii* to various fermentation conditions, GC–MS and LC–MS/MS were performed. The details of each fermentation condition could be found in Table 1.

The sampling and quenching were performed according to the methods described by Xia et al. [55] with slight modifications. For each sampling time point (18 and 30 h), 20 mL culture sample was taken from the fermentation broth and immediately transferred to a 50-mL tube containing 20 mL 60% methanol solution pre-chilled at − 40 °C. The whole procedure from sampling to quenching of metabolism was completed within 10–15 s. Then the mixture was centrifuged at 5000 rpm for 5 min and the supernatant was removed. After centrifugation, the cells were subsequently washed with 10 mL 0.9% (w/v) NaCl solution, twice. The samples were frozen at − 80 °C until further processing.

Then, the extraction, determination, and analysis of intracellular metabolites were performed according to the previous methods [55]. The metabolites including sugar phosphate intermediates of Embden–Meyerhof–Parnas (EMP) and pentose phosphate (PP) pathway were detected by LC–MS/MS. All the experimental data were obtained from five replicates for each treatment.

The peak area of each metabolite was normalized by the internal standard succinic acid-d_4 and biomass in GC–MS analysis. Absolute metabolite concentrations determined by LC–MS/MS were normalized by the biomass and internal standard D-sorbitol-$^{13}C_6$. Both of the normalized data from GC–MS and LC–MS/MS were combined together for the final analysis [51]. The relative abundance matrix of all the identified metabolites at each sampling time point was imported into SIMCA-P package (version 11.5, Umetrics AB, Umea, Sweden) for principal component analysis (PCA).

WGCNA network construction

A metabolic correlation network was established from the GC/MS and LC–MS/MS datasets by calculating weighted Pearson's correlation matrices corresponding to metabolite abundance, followed by creating the networks according to the standard procedure of WGCNA [45, 58]. Briefly, connection strength matrices were created from the transformation of weighted correlation matrices by a power function, and then used to calculate topological overlap (TO). Then the metabolites with highly similar correlation relationships were grouped into the same modules through hierarchical clustering based on the results of TO. Subsequently, average linkage hierarchical clustering was performed to obtain metabolite dendrograms. The module assignment determined by the Dynamic Tree Cut of WGCNA was distinguished with the color row underneath the dendrograms. The modules with correlation $r \geq 0.6$ or $r \leq -0.6$ with statistical significance p value less than 0.05 were extracted for further investigation. Hub metabolites were screened by high connectivity with other metabolites (≥ 5) in the modules strongly associated with phenotype [40].

Quantitative iTRAQ–LC–MS/MS proteomic analysis

For quantitative proteomic analysis, the cells grown under the control and N_2–PE–YE–$Ca(OH)_2$ condition (Table 1) at 18 h (each sample with two biological replicates) were collected by centrifugation (12,000 *g* for 10 min at 4 °C) and frozen in liquid nitrogen, respectively. The quantitative proteomics experiment procedure was the same as previous report [22], including: (1) protein extraction, digestion, and iTRAQ labeling. Each sample was labeled separately with two of the four available tags (control: 113, 115; N_2–PE–YE–$Ca(OH)_2$: 117, 121); (2) LC–MS/MS analysis; and (3) proteomic data analysis. The raw MS/MS data were converted to MASCOT generic format (.mgf) files via

Proteome Discoverer 1.4 (Thermo Fisher Scientific Inc., MA, USA). Protein Pilot 5.0 (AB Sciex, Foster City, CA, USA) was used for deep proteome analysis and protein quantitation analysis with MASCOT generic format (.mgf) files as input and 1% FDR for proteins and peptides. After that, the raw peptide identification results were classified according to the SWISS-PROT online database (http://www.uniprot.org). The proteins with the average ratio-fold change ≥ 2 or ≤ 0.5 with p value < 0.05 were confidently considered as differentially expressed proteins, and then subjected to further functional and pathway analysis.

Results and discussion

Fermentation characterizations of *L. delbrueckii* under different fermentation conditions

As shown in Fig. 1, the effects of five fermentation conditions (Table 1) on D-LA production were investigated in 7.5-L fermenter, respectively. The results showed that the biomass synthesis, D-LA accumulation, and glucose consumption were all superior to the control under the conditions of N_2, PE–YE, $Ca(OH)_2$, and N_2–PE–YE–$Ca(OH)_2$, respectively. However, they were inferior to the control under the NaOH condition. It would indicate that: (1) the anaerobic condition (inletting N_2 into the medium) would be more suitable for the cell growth and D-LA production; (2) in regard to neutralizing agents, $Ca(OH)_2$ would be the best choice, followed by $CaCO_3$, while NaOH obviously

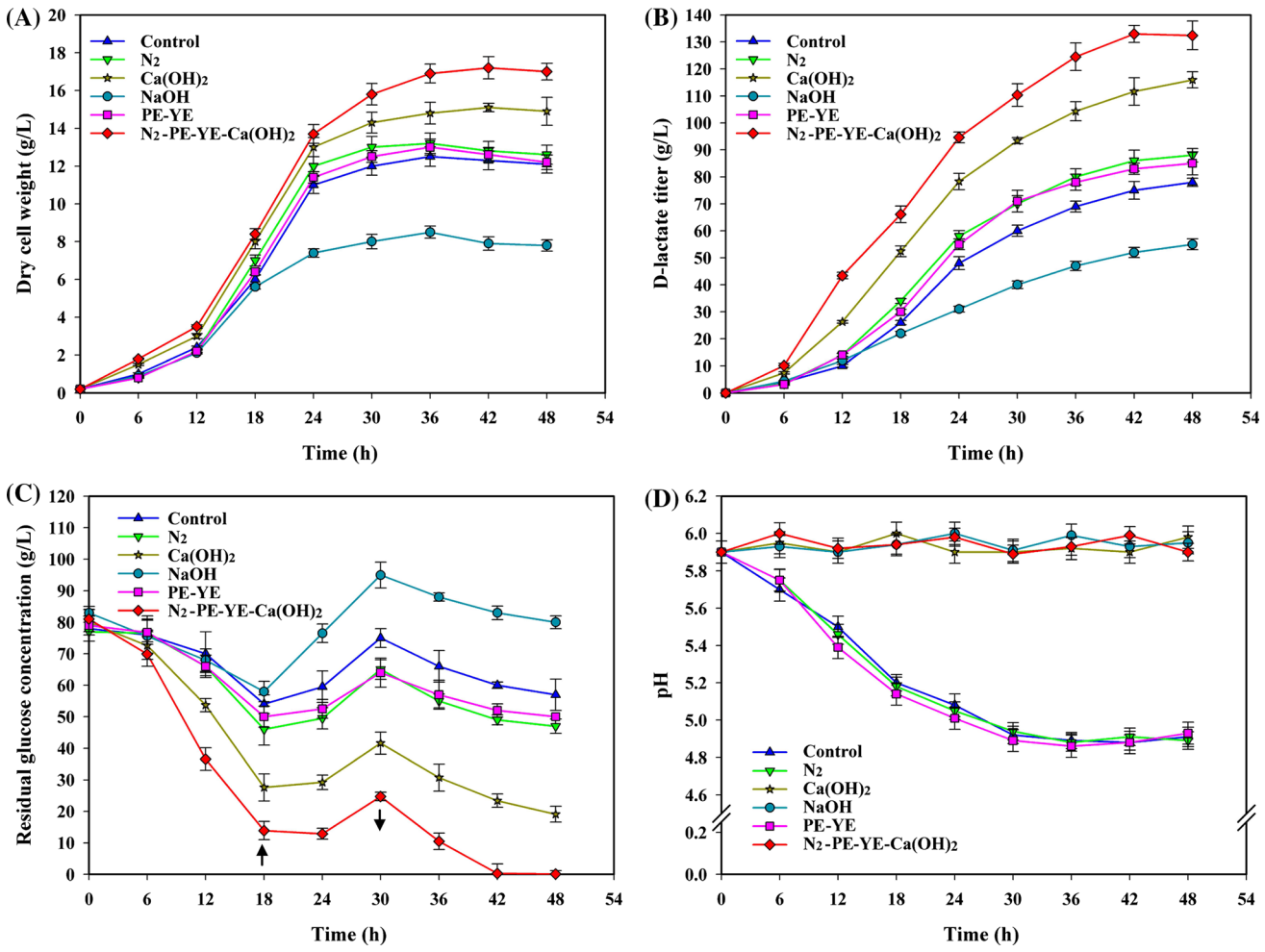

Fig. 1 Fermentation time course of *L. delbrueckii* under various fermentation conditions. **a** Dry cell weight; **b** D-LA titer; **c** residual glucose concentration; **d** pH value. The arrows represent the starting and terminal time points of glucose feeding, respectively. Values and error bars represent the averages and standard deviations obtained from three independent replicates

inhibited the cell growth and D-LA production, although it could adjust pH in the optimal range of 5.9–6.0 (Fig. 1d); (3) the combination of peptone and yeast extract as the nitrogen sources were better than beef extract for D-LA production. Besides, the dynamic measurement showed that the conditions mentioned above did not affect the optical purity of D-LA production. Furthermore, the formation of side products was not observed in our experiments, which indicated that our strain specially produced D-LA without side products. Finally, under the combined condition (N_2–PE–YE–$Ca(OH)_2$), *L. delbrueckii* produced 133 g/L D-LA (1.71-fold increase compared with the control), with a volumetric productivity of 3.17 g/(L h) (1.95-fold increase compared with the control), a yield of 98%, and an optical purity of 99.6%.

Effects of different fermentation conditions on metabolomic profiles

A total of 90 intracellular metabolites, including 80 metabolites by GC–MS analysis and 10 sugar phosphates by LC–MS/MS analysis (Supplementary Materials A: Table S1), were identified for all fermentation conditions (a total of 60 samples) at the different sampling times (i.e., 18 and 30 h). According to the PCA score plots of intracellular metabolic profiles (Fig. 2), several obvious features could be observed: (1) clustering of the same treated samples was clearly observed and well-separated metabolomic profiles between different treated samples were detected; (2) the distances between different treated samples in the PCA score plots might reflect the metabolomic differences of different treated samples. At 18 h, obvious metabolomic differences were observed under the conditions of N_2, $Ca(OH)_2$, and N_2–PE–YE–$Ca(OH)_2$ compared with the control, respectively (Fig. 2a). While at 30 h, significant metabolomic differences were detected under the conditions of PE–YE, NaOH, $Ca(OH)_2$, and N_2–PE–YE–$Ca(OH)_2$, respectively (Fig. 2b); (3) among various fermentation conditions, $Ca(OH)_2$ seemed to be the major discriminating factor as profiles under $Ca(OH)_2$ and N_2–PE–YE–$Ca(OH)_2$ conditions were well-separated in the PCA plots in both time points.

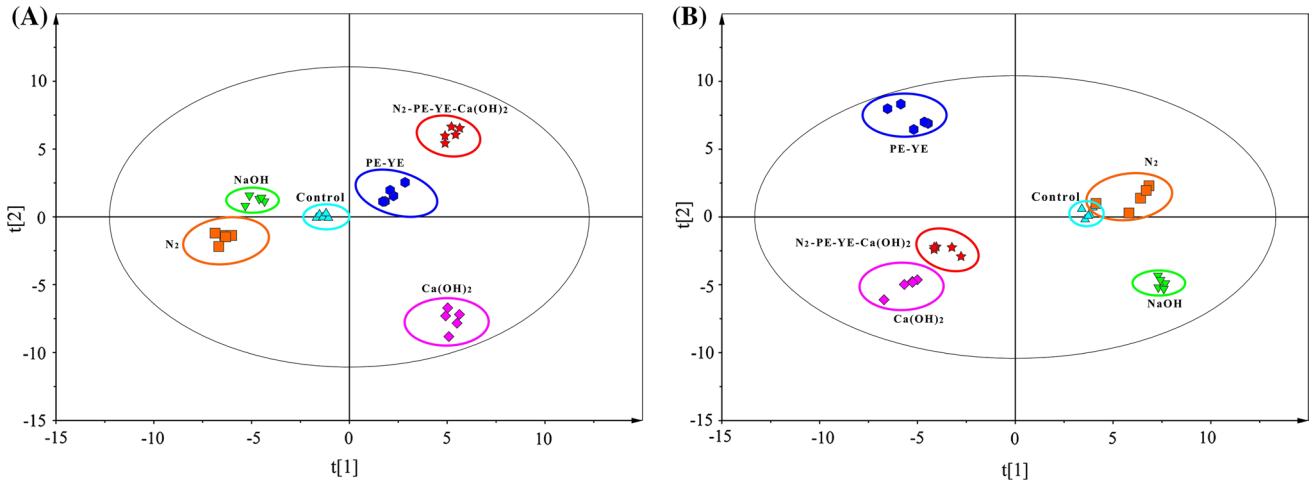

Fig. 2 PCA analysis of GC–MS and LC–MS/MS metabolomic datasets. **a** 18 h after inoculation; **b** 30 h after inoculation. T1 and T2 are referred as the scores of projection 1 and 2 in PCA analysis, respectively

Table 2 Associated modules under different conditions in this study in Fig. 3

Time	Module	Condition	Compound	*r*	*p*
18 h	M1-18 h	N_2–PE–YE–$Ca(OH)_2$	15	0.65	4.00E−04
	M2-18 h	N_2	7	0.78	4.00E−07
	M3-18 h	N_2–PE–YE–$Ca(OH)_2$	7	0.64	5.00E−4
		$Ca(OH)_2$	7	0.61	1.00E−3
	M4-18 h	N_2–PE–YE–$Ca(OH)_2$	18	0.89	8.00E−10
	M5-18 h	NaOH	16	0.91	6.00E−12
30 h	M1-30 h	PE–YE	12	0.85	2.00E−05
	M2-30 h	N_2–PE–YE–$Ca(OH)_2$	8	0.69	1.00E−04
	M3-30 h	NaOH	26	−0.6	5.00E−04
	M4-30 h	$Ca(OH)_2$	14	0.68	4.00E−05

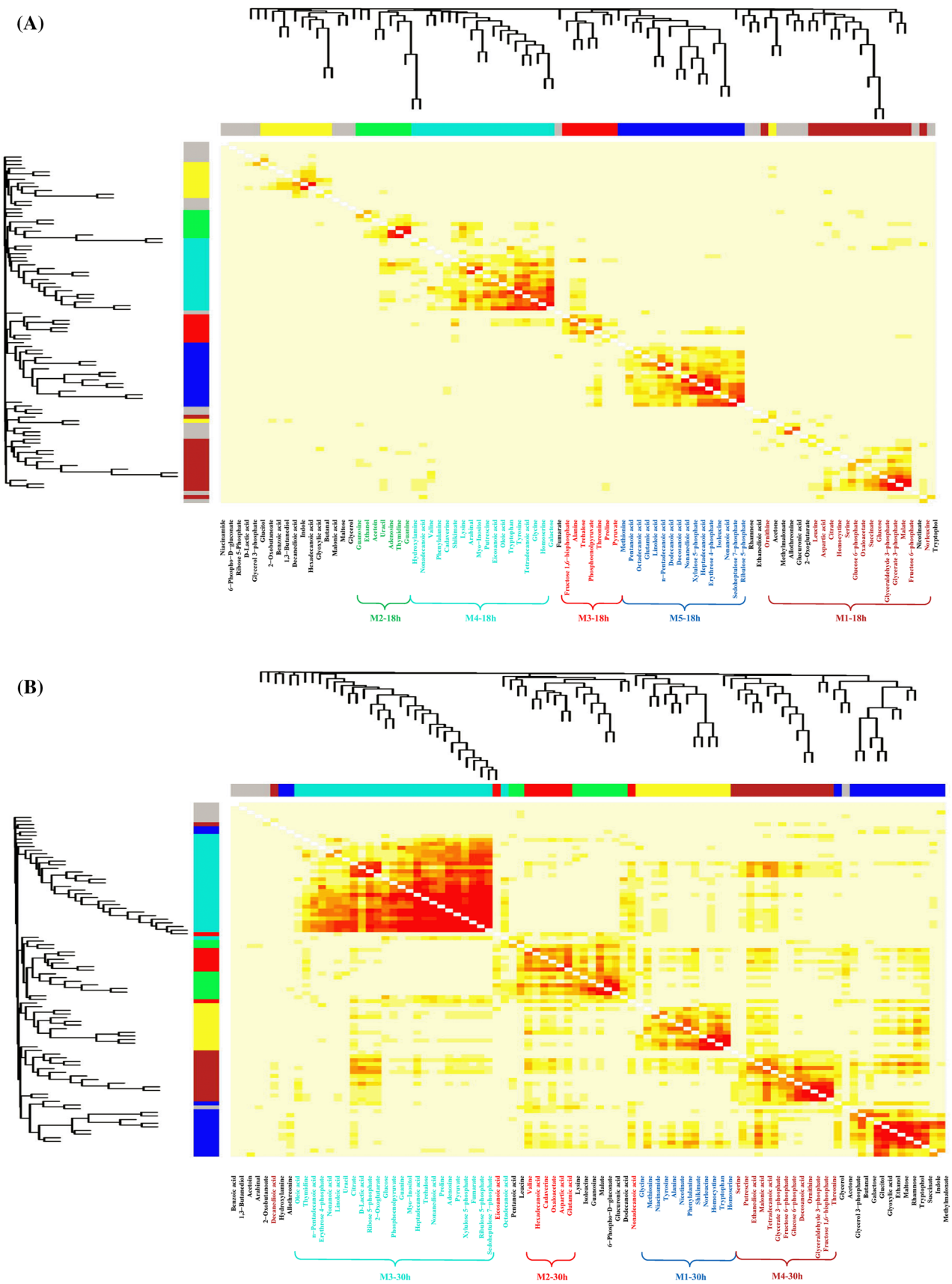
(A)
Niacinamide
6-Phospho-D-gluconate
Ribose 5-Phosphate
Butyric acid
Glycerol 3-phosphate
Glucitol
2-Oxobutanoate
Butanoic acid
1,3-Butanediol
Decanedioic acid
Indole
Hexadecanoic acid
Glyoxylic acid
Butanal
Malonic acid
Maltose
Glycerol
Guanosine
Ethanol
Acetoin
Uracil
Adenosine
Thymidine
Guanine
Hypoxanthine
Nonadecanoic acid
Valine
Phenylalanine
Galactitol
Shikimate
Lysine
Arabinol
Myo-Inositol
Putrescine
Eicosanoic acid
Oleic acid
Tryptophan
Tyrosine
Tetradecanoic acid
Glycine
Homoserine
Galactose
Fumarate
Fructose 1,6-bisphosphate
Alanine
Threonine
Phosphoenolpyruvate
Threonine
Proline
Pyruvate
Methionine
Pentanoic acid
Octadecanoic acid
Glutamic acid
Linoleic acid
n-Pentadecanoic acid
Dodecanoic acid
Hexanoic acid
Nonanoic acid
Xylulose 5-phosphate
Heptadecanoic acid
Erythrose 4-phosphate
Isoleucine
Nonanoic acid
Sedoheptulose 7-phosphate
Ribulose 5-phosphate
Ribose
Ethanolamine
Ornithine
Acetone
Methylmalonate
Allothreonine
Gluconic acid
2-Oxoglutarate
Leucine
Citrate
Aspartic acid
Homocysteine
Citrate
Serine
Glucose 6-phosphate
Oxaloacetate
Succinate
Glucose
Glyceraldehyde 3-phosphate
Glycerate 3-phosphate
Malate
Fructose 6-phosphate
Norleucine
Tryptophol
M2-18h
M4-18h
M3-18h
M5-18h
M1-18h
(B)
Benzoic acid
1,3-Butanediol
Acetoin
Acetic acid
2-Oxobutanoate
Decanedioic acid
Hydroxylamine
Methylamine
Oleic acid
Thymidine
n-Pentadecanoic acid
Erythrose 4-phosphate
Nonanoic acid
Linoleic acid
Uracil
Citric acid
D-Lactic acid
Ribose 5-phosphate
2-Oxoglutarate
Glucose
Ethanol
Phosphoenolpyruvate
Guanine
Myo-Inositol
Heptadecanoic acid
Threonine
Nonanedioic acid
Proline
Adenosine
Pyruvate
Xylulose 5-phosphate
Fumarate
Ribulose 5-phosphate
Sedoheptulose 7-phosphate
Eicosanoic acid
Octadecanoic acid
Pentanoic acid
Leucine
Valine
Hexadecanoic acid
Cadaverine
Oxaloacetate
Arachidic acid
Glutamic acid
Lysine
Isoleucine
Guanosine
Malate
6-Phospho-D-gluconate
Gluconic acid
Butanoic acid
Nonadecanoic acid
Glycine
Methionine
Niacinamide
Tyrosine
Alanine
Nicotinate
Phenylalanine
Shikimate
Norleucine
Homocysteine
Tryptophan
Histidine
Serine
Putrescine
Ethanolic acid
Malonic acid
Tetradecanoic acid
Glycerate 3-phosphate
Fructose 6-phosphate
Glucose 6-phosphate
Dodecanoic acid
Ornithine
Glyceraldehyde 3-phosphate
Fructose 1,6-bisphosphate
Thymidine
Glycerol
Acetone
Glycerol 3-phosphate
Butanal
Galactose
Glucitol
Glyoxylic acid
Malonic acid
Maltose
Rhamnose
Tryptophol
Succinic acid
Indole
Methylmalonate
M3-30h
M2-30h
M1-30h
M4-30h

◂**Fig. 3** WGCNA of metabolomic profiles of *L. delbrueckii* under various fermentation conditions. **a** 18 h after inoculation; **b** 30 h after inoculation. The heat maps depict the topological overlap (TO) matrix among 90 metabolites in the analysis. Light color represents low TO and progressively darker red color represents higher TO. Blocks of darker colors along the diagonal are the modules. The metabolites dendrogram and module assignment are also shown along the left side and the top. The modules highly associated with any given treatment ($r \geq 0.6$ or $r \leq -0.6$ and p value < 0.05) are indicated with their metabolites within the modules in different colors, and the correlation coefficients and related p values are listed in Table 2

WGCNA correlation network construction

To further search the differences of intracellular metabolism, a WGCNA network analysis was performed for all fermentation conditions based on the GC–MS and LC–MS/MS datasets. WGCNA is a correlation-based and unsupervised computational method to describe and visualize correlation patterns of data points [58], and has been widely applied to metabolomic data of bacteria under various conditions [45]. According to the standard protocol, five and four distinct metabolic modules were identified successfully at 18 and 30 h, respectively. The detailed information of each metabolic module is described in Table 2 and Fig. 3.

As shown in Fig. 3, the great differences of metabolites within each module could be found at different time points. At 18 h, most of metabolites in the M2-18 h module, which was significantly associated with N_2 condition, were mainly involved in nucleotide metabolism (i.e., uracil, guanosine, etc.), indicating that nucleotide metabolism might be influenced by anaerobic condition seriously. Oxygen is unable to cause any damage to the cell directly, but during the cellular processes, O_2 could partially transform into the reactive O_2 species (O^{2-}, OH,·and H_2O_2), which have high oxidizing potentials and thus lead to cellular oxygen toxicity [32]. In lactic acid bacteria (LAB), the toxicity of oxygen is generally attributed to the attachment of reactive oxygen species to proteins, lipids, and nucleic acids, thereby causing aging and cell death [50]. It has been reported that the high dissolved oxygen (DO) would result in the accumulation of H_2O_2, which caused the early entry into stationary phase and markedly reducing the biomass production of *L. delbrueckii* [30]. So the anaerobic condition would reduce the oxygen toxicity to cellular metabolism, such as nucleotide metabolism (just as shown in our metabolomic data), and be more beneficial for cell growth in the D-LA fermentation.

In the M3-18 h module, several intermediate metabolites of glycolysis (i.e., fructose 1, 6-bisphosphate and phosphoenolpyruvate) and amino acids (i.e., proline, threonine, alanine, etc.) were highly related with $Ca(OH)_2$ condition. Generally, LAB are neutrophiles (the optimal growth pH was between 5 and 9), low pH environment will cause the internal acidification, reduce the activity of acid-sensitive enzymes, and damage proteins and DNA [50]. Serrazanetti et al. [44] found that acid stress would induce a metabolic shift in *L. sanfranciscensis*, such as reduction of sugar consumption and primary carbohydrate metabolism, and changes of amino acid metabolism. In this work, pH was maintained at the optimal value (5.9–6.0) under the $Ca(OH)_2$ condition, but was dropped to 5.2 at 18 h and 4.7 at 30 h under the control condition (Fig. 1d). The change of pH also resulted in a metabolic shift of central carbon and amino acid metabolism in our strain, which was similar to previous report [44]. The more suitable pH environment under the $Ca(OH)_2$ condition would prompt the glucose consumption and amino metabolism, which were in favor of cell growth and D-LA synthesis.

Unlike $Ca(OH)_2$ condition, several metabolites (linoleic acid, octadecanoic acid, dodecanoic acid, etc.) existed in fatty acid metabolism which were significantly associated with the NaOH condition (M5–18 h). Although using NaOH as a neutralizing agent could keep the pH at the optimal value, the cell growth and D-LA production were much lower than that of $Ca(OH)_2$ (Fig. 1). Obviously, pH was not the dominant factor under the NaOH condition. We speculated that Na^+ stress was the main reason for hampering cell growth and D-LA production. Glaasker et al. [17] found that KCl and NaCl dramatically inhibited the growth of *L. plantarum*, which was unable to respond adequately to osmotic stress by the accumulation of K^+ or Na^+. Guerzoni et al. [20] found that Na^+ salt stress would alter the cellular fatty acid composition, and increase the proportion of unsaturated fatty acid. In this study, the inhibition of cell growth and alteration of fatty acid composition under the NaOH condition were also observed, which resulted in the lower D-LA production.

It was worth noting that most of the metabolic modules (M1-18 h, M3-18 h, and M4-18 h) could be found in the N_2–PE–YE–$Ca(OH)_2$ condition. The corresponding metabolites located in these modules were mainly involved in central carbohydrate metabolism, amino acid metabolism, and fatty acid metabolism, which indicated that the combined condition caused huge metabolic flux redirection. It was not difficult to understand that the N_2–PE–YE–$Ca(OH)_2$ condition caused huge metabolic flux redirection, since the N_2–PE–YE–$Ca(OH)_2$ condition was the optimal combination of above mentioned conditions, which avoided oxygen toxicity, acid stress, and salt stress to the cells. Less cell damage would facilitate the cell growth and D-LA production (Fig. 1).

At 30 h, no module was associated with N_2 condition, while each of other four conditions had one significant metabolic module, respectively. Specifically, extremely differential metabolism was observed under the NaOH condition, as M3-30 h module, associated with the NaOH condition, contained up to 26 metabolites, which involved central

carbohydrate metabolism, amino acid metabolism, fatty acid metabolism, and nucleotide metabolism, suggesting the complexity of the cellular responses to the NaOH condition. Na^+ concentration had nearly doubled from 18 to 30 h, which caused the medium in a higher osmolality state. The effects of high-osmolality on amino acid metabolism and fatty acid metabolism in LAB have been reported [18, 20]; however, it remained unclear on central carbon metabolism and nucleotide metabolism. With the accumulation of D-LA, besides osmotic stress, lactate molarity might play another dominant role, as the generated molarity of Na^+ lactate is two-fold of Ca^{2+} lactate when neutralizing the same molarity of D-LA. It has been reported that the growth of LAB was usually inhibited by the accumulation of lactate [16] and high concentration of sodium lactate would inhibit the cell growth and D-LA production [35]. Hence, higher osmotic stress and lactate molarity might be the main reasons for significant inhibition of bacteria growth and D-LA production under the NaOH condition.

Finally, the metabolites within M1-30 h module were involved in amino acids, such as glycine, tryptophan, and methionine, which might result from the intracellular nitrogen metabolic disturbance caused by the substitution of beef extract with peptone and yeast extract. No significant metabolic differences between the PE–YE and control conditions were observed at 18 h, but amino acid metabolism changed significantly at 30 h. The supply of amino acids was sufficient under both conditions at 18 h. With the cell growth and metabolism, several essential amino acids (such as glycine, tryptophan, and methionine) were depleted under the control condition, but still enough under the PE–YE condition at 30 h (Fig. S2). The depletion of these amino acids would cause nitrogen starvation, which resulted in the limitation of protein synthesis [50]. Therefore, the sufficient supply of essential amino acids might be the main reason for higher D-LA production under the PE–YE condition compared with the control.

Hub metabolites have a high degree of connectivity in biological interaction networks and are thus assumed to have high biological importance [56]. Assuming hub metabolites with connectivity greater than 5, six hub metabolites (fructose 6-phosphate, glycerate 3-phosphate, ornithine, trehalose, oleic acid, and eicosanoic acid) were identified to be significantly associated with N_2–PE–YE–$Ca(OH)_2$ condition at 18 h, and two hub metabolites (aspartic acid and glutamic acid) at 30 h, based on the WGCNA analysis (Fig. 4). At 18 h, (1) in M1-18 h module, three hub metabolites, fructose 6-phosphate, glycerate 3-phosphate, and ornithine, were identified and connected to several other metabolites (Fig. 4a). Fructose 6-phosphate and glycerate 3-phosphate were the intermediate metabolites of glycolysis, which directly correlated with D-LA synthesis. Ornithine was the product of arginine degradation through the arginine deiminase (ADI) pathway, which has been confirmed

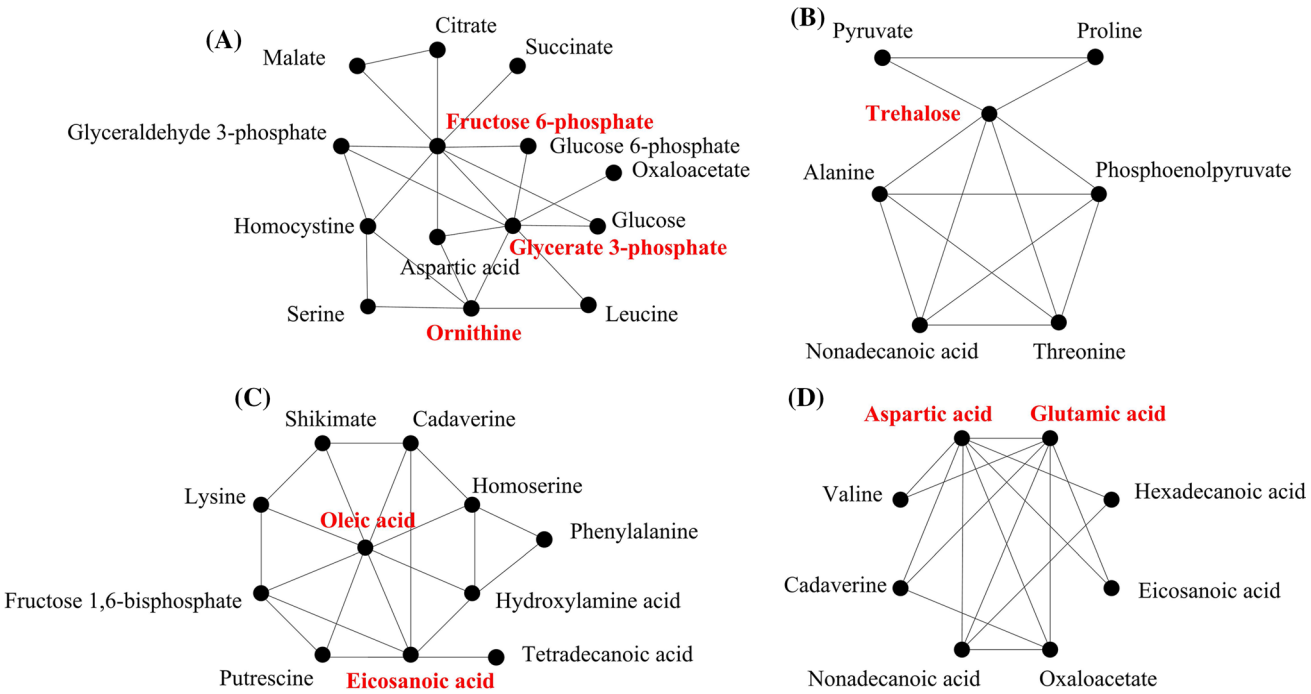

Fig. 4 Hub metabolites and their metabolic profiles as represented by node and edge graph. **a** Fructose 6-phosphate, glycerate 3-phosphate and ornithine for M1-18 h module; **b** trehalose for M3-18 h module; **c** oleic acid and eicosanoic acid for M4-18 h module; **d** aspartic acid and glutamic acid for M2-30 h. The hub metabolites are identified under the N_2–PE–YE–$Ca(OH)_2$ condition

to play an important role in pH homeostasis [36]; (2) in M3-18 h module, the hub of trehalose (Fig. 4b) might serve as an important osmoprotectant and stress protectant [41]. The lower relative abundance of trehalose (Supplementary Materials B: Fig. S1) might reflect lower cellular osmotic stress under N_2–PE–YE–$Ca(OH)_2$ condition compared with the control; (3) the hubs of oleic acid and eicosanoic acid (Fig. 4c) were located in M4-18 h module. In the previous reports, oleic acid has been found to be a necessary growth factor in *L. delbrueckii* [39], and the intracellular fatty acids (such as oleic acid) of *L. helveticus* were altered when suffered to salt, acid, oxidative, and thermal stresses [20]. Here, the combined condition also resulted in alteration of intracellular fatty acid composition, such as the increase of oleic acid and eicosanoic acid (Supplementary Materials B: Fig. S1). At 30 h, aspartic acid and glutamic acid were identified as hub metabolites (Fig. 4d). In fact, aspartic acid and glutamic acid not only served as nitrogen source, but also regulated intracellular pH through decarboxylase pathway [36]. Therefore, these identified hub metabolites might serve as obvious biomarkers in the D-LA overproduction.

Proteomic analysis

Overview of proteomic analysis

According to the results of fermentation characterizations, the combined condition of N_2–PE–YE–$Ca(OH)_2$ achieved the highest D-LA production (133 g/L) (Fig. 1). Meanwhile, WGCNA analysis showed significantly different metabolism of *L. delbrueckii* under N_2–PE–YE–$Ca(OH)_2$ condition at 18 h compared with the control (Fig. 3a). Actually, because of the "combined effects" of N_2–PE–YE–$Ca(OH)_2$ condition, the changes of intracellular metabolism were caused by various conditions, so it was difficult to establish the relationship between the N_2–PE–YE–$Ca(OH)_2$ condition and metabolomic data. Hence, to further uncover the mechanisms of D-LA overproduction, a quantitative iTRAQ–LC–MS/MS proteomic analysis was then employed to analyze the proteomic differences between N_2–PE–YE–$Ca(OH)_2$ condition and the control at 18 h.

Based on the analysis with Protein Pilot 5.0 search engine, a total of 183,740 spectra, 78,435 spectra identified,

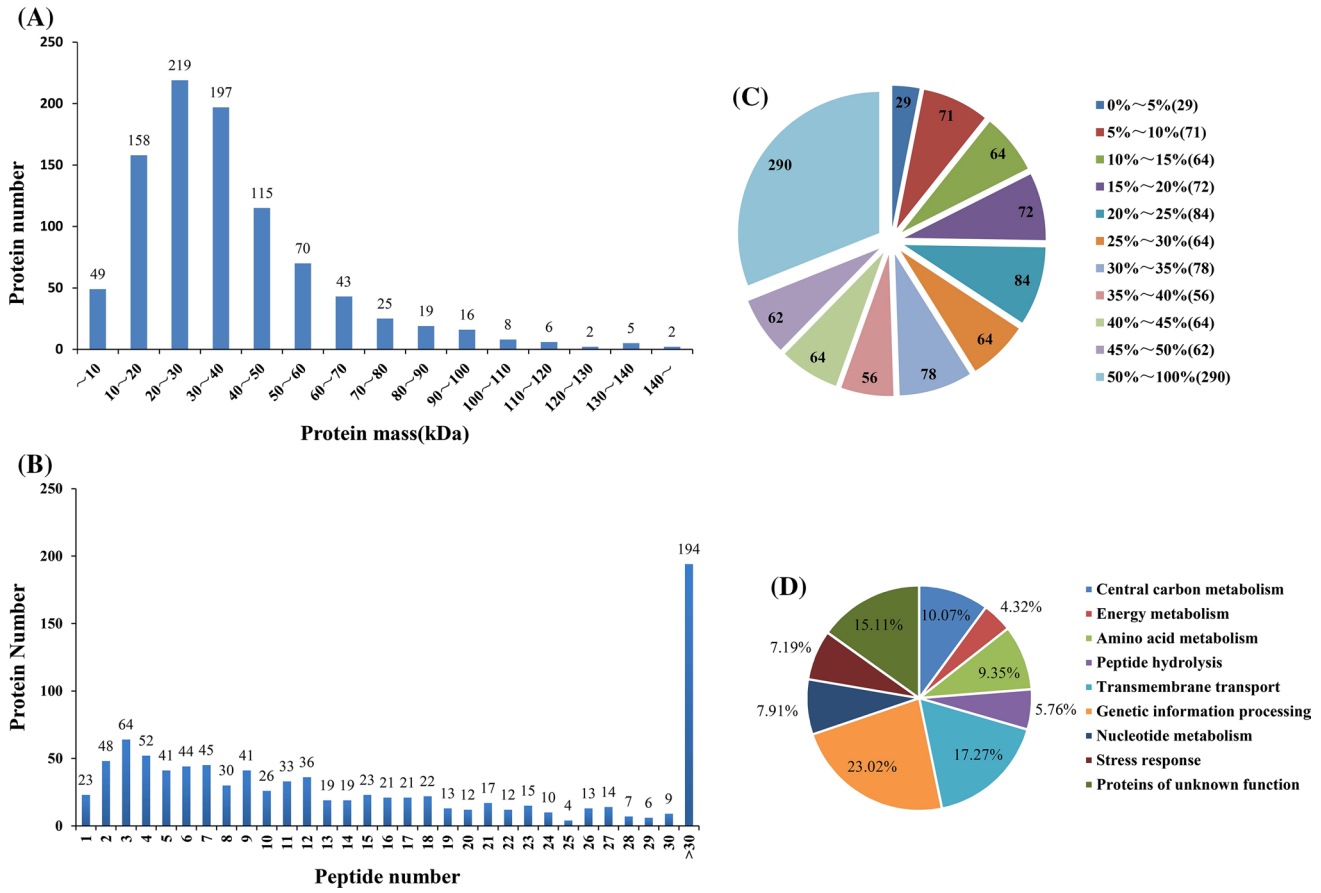

Fig. 5 Proteome of *L. delbrueckii* and functional category of differential expression proteins identified in this study. **a** Distribution of proteins with different molecular weights; **b** number of peptides that match to proteins identified by Protein Pilot 5.0; **c** coverage of proteins by the identified peptides; **d** functional category coverage of differentially expressed proteins

32,951 distinct peptides, 1422 proteins before grouping, and 934 proteins were acquired. The 934 detected proteins (Supplementary Materials A: Table S2) accounted for approximately 61.5% of the 1519 predicted proteins in the *L. delbrueckii* genome [49]. In terms of protein molecular weight (MW) distribution, there were 738, 173, and 23 proteins with a mass of 10–50 kDa, 50–100 kDa, and more than 100 kDa, respectively (Fig. 5a). The distribution of peptide numbers is shown in Fig. 5b, and a large number of proteins with more than 30 peptides were observed. In addition, most of the proteins were identified with high-quality peptide coverage, among which 89.3% of the total identified proteins had more than 10% peptide coverage and 74.7% of them were found with more than 20% peptide coverage (Fig. 5c). According to the abundance of each identified protein, a total of 139 differential expression proteins ($\geq$ two-fold change and adjusted $p < 0.05$) were found under the N_2–PE–YE–$Ca(OH)_2$ condition, among which 97 and 42 proteins were up- and down-regulated, respectively. The detailed information of the up- and down-regulated proteins is listed in supplementary material (Supplementary Materials A: Table S3 and Table S4). They were classified into nine functional groups by their cellular roles, mainly including central carbon metabolism, energy metabolism, amino acid metabolism, peptide hydrolysis, transmembrane transport, genetic information processing, nucleotide metabolism, stress response, and proteins of unknown function (Fig. 5d), suggesting the complexity of the cellular metabolism under the N_2–PE–YE–$Ca(OH)_2$ condition.

Central carbon metabolism and energy metabolism

Central carbon metabolism represents the backbone of the cellular metabolism and provides the energy and precursors for the cell growth and the synthesis of target products. In this study, proteomic analysis showed that the expression levels of two key enzymes involved in EMP pathway, i.e., ATP-dependent 6-phosphofructokinase (Pfk1, Ldb0838) and pyruvate kinase (Pyk, Ldb0839) exhibited 10.21- and 8.31-fold increases under the N_2–PE–YE–$Ca(OH)_2$ condition, respectively. Meanwhile, fructose-bisphosphate aldolase (Fba, Ldb1544), NADP-dependent glyceraldehyde-3-phosphate dehydrogenase (GapN, Ldb1179), and enolase (Eno, Ldb1294) were also up-regulated, suggesting that the EMP pathway was strengthened. The up-regulated EMP pathway not only supplied more precursors for D-LA synthesis, but also generated more phosphoenolpyruvate for phosphotransferase system (PTS), which was the dominant glucose transporter in *Lactobacilli* [9]. Moreover, it was worth noting that D-lactate dehydrogenase (LdhA, Ldb0101), an important enzyme, directly participating in the bioconversion of pyruvate to D-LA, achieved a 12.78-fold increase under the N_2–PE–YE–$Ca(OH)_2$ condition, which was an important reason for the remarkable improvement of D-LA production.

In PP pathway, glucose-6-phosphate dehydrogenase (Gpd, Ldb1611), ribose-5-phosphate isomerase A (RpiA, Ldb0531), ribulose-phosphate 3-epimerase (Rpe, Ldb0530) and phosphoketolase (Ldb0534) were significantly up-regulated under the N_2–PE–YE–$Ca(OH)_2$ condition, implying that PP pathway was also enhanced. In fact, glucose could be oxidized through PP pathway to generate NADPH for the antioxidant system and biosynthesis [59], and ribose-5-phosphate for the synthesis of nucleotides [8]. The increased levels of PP pathway enzymes would be beneficial for the cell growth.

The precursor of D-LA synthesis is the intermediate metabolite of EMP pathway, so higher flux through EMP pathway would provide more precursors for D-LA synthesis. Meanwhile, PP pathway provides NADPH and precursors of nucleotides for cell growth [8, 59]. Since the production of D-LA was predominantly growth-associated [3], the higher flux through PP pathway would also beneficial for D-LA production. Papagianni and his colleagues [37, 38] promoted the flux through EMP pathway in *L. lactis* by metabolic engineering methods and enhanced the bacteria growth by optimization of culture conditions, and then the productivity of lactic acid was dramatically increased. Hence, higher flux through EMP and PP pathway would increase the D-LA production.

In regard to TCA cycle, it has been reported that TCA cycle was incomplete in multiple auxotrophic *Lactobacilli* [33]. In this study, only two enzymes in TCA cycle, fumarate hydratase (FumC, Ldb2086) and fumarate reductase (Ldb0795), were identified in our proteomic analysis, but both of them showed no significant abundance changes. Additionally, both pyruvate oxidase (Pox1, Ldb2213) and phosphate acetyltransferase (Pta, Ldb0643) were down-regulated, which converted pyruvate to acetyl-CoA together and competed pyruvate with D-LA. Acid stress could induce the expression of Pox1 and Pta in *L. delbrueckii* and *L. rhamnosus* [26, 57]. Therefore, the decreased expression levels of Pox1 and Pta might result from the higher pH under the N_2–PE–YE–$Ca(OH)_2$ condition, and reduce the competition of pyruvate for D-LA synthesis.

Besides, five proteins related with F_0F_1-ATP synthase (F_0F_1-ATPase) were down-regulated under the N_2–PE–YE–$Ca(OH)_2$ condition, containing F_0F_1-ATPase subunit alpha (AtpA, Ldb0709), F_0F_1-ATPase subunit beta (AtpD, Ldb0711), F_0F_1-ATPase subunit gamma (AtpG, Ldb0710), F_0F_1-ATPase subunit a (AtpB, Ldb0705), and F_0F_1-ATPase subunit b (AtpF, Ldb0707). F_0F_1-ATPase is a multimeric enzyme that can either synthesize ATP using protons flowing from the environment to the cell, or conversely, export protons out of the cell using the energy

provided by ATP hydrolysis [26]. F_0F_1-ATPase was responsible for pH homeostasis in LAB [23]. Higher pH at exponential phase led to the down-regulation of F_0F_1-ATPase subunit alpha in *L. rhamnosus* [26], which was similar to our results. According to the above analysis, more suitable pH environment under the N_2–PE–YE–$Ca(OH)_2$ condition might reduce the ATP cost for exporting protons by F_0F_1-ATPase, and more ATP could be used for the synthesis of building blocks and D-LA.

Amino acid metabolism and peptide hydrolysis

Amino acid metabolism plays a significant role in LAB, such as pH homeostasis, generation of energy or reducing power, and resistance to stress [7]. Obvious changes of several enzymes involved in amino acid metabolism have been shown under the N_2–PE–YE–$Ca(OH)_2$ condition. For example, S-adenosylmethionine (SAM) synthase (MetK, Ldb1575) was detected at a higher abundance. Methionine plays a central role in bioconversion among sulfur amino acids, and could be transformed to cysteine through SAM cycle [7]. Similar to SAM synthase, aspartate-ammonia ligase (AsnA, Ldb1194) and glutamine synthetase (GlnA, Ldb1472) were also up-regulated, which could catalyze the synthesis of asparagine and glutamine, respectively. Asparagine and glutamine play important roles in nitrogen storage and distribution [14]. In addition, two aminotransferases [aromatic amino acid aminotransferase (Ldb1263) and branched-chain amino acid aminotransferase (IlvE, Ldb1305)] were also up-regulated. In most LAB, aminotransferase was the initial enzyme of aromatic amino acid and branched-chain amino acid metabolism [42], which initiated the aromatic amino acid and branched-chain amino acid catabolism. The higher abundances of Ldb1263 and IlvE suggested that aromatic amino acid and branched-chain amino acid metabolism were more active, which provided more precursors and energy for building blocks related with central carbon metabolism.

Lactobacilli generally have 6–14 amino acid auxotrophies, so it is necessary to assimilate amino acids and peptides from environment, and liberate essential amino acids from peptides by intracellular peptidase system [4]. Klotz et al. [25] also found that *S. inulinus* was auxotrophic for various amino acids, such as methyl-branched amino acids and aromatic amino acids, and free amino acids were the limiting factor for the lactic acid production. In this study, eight peptidases, i.e., aminopeptidase N (PepN, Ldb2080), aminopeptidase C (PepC, Ldb1730), proline iminopeptidase (PepPN, Ldb1909), X-Pro dipeptidase (PepP, Ldb1429), endopeptidase (PepO1, Ldb0218), dipeptidase (PepD1, Ldb0511; PepD2, Ldb2063), and oligoendopeptidase F (PepF, Ldb2034) were present at higher levels under the N_2–PE–YE–$Ca(OH)_2$ condition, suggesting that more peptides were transported into cells and released by peptidases to supply essential amino acids for protein synthesis, which were in favor of cell growth and D-LA production.

Transmembrane transport

LAB expressed a lot of transporters for nutrient uptake. In this study, numerous transporters were observed with differential expression under the N_2–PE–YE–$Ca(OH)_2$ condition compared with the control, including ten ABC transporters, eight proteins in PTS system, two cation transporters, two phosphate transporters, one branched-chain amino acid transport system carrier protein, and one Na^+/H^+ antiporter. In PTS system, phosphocarrier protein HPr (PtsH, Ldb0576) and glucose-specific enzyme IIA component (Ldb2065 and Ldb1823) were significantly up-regulated, and several other sugar-specific PTS components (Ldb1799, Ldb1800, Ldb1801, Ldb2040, and Ldb1771) were down-regulated. Under the optimal conditions and glucose-rich media, HPr inhibits PTSs for carbohydrates other than glucose, preventing their transport into the cell [36]. The higher expression of glucose-specific PTS promoted the glucose uptake from medium for D-LA synthesis. Additionally, several proteins related with amino acid and peptide transport were up-regulated. In detail, amino acid ABC transporter (Ldb0169) and branched-chain amino acid transport system carrier protein (BrnQ, Ldb0483) showed 6.95-fold and 6.71-fold increase, respectively. Oligopeptide ABC transporters (OppCII, Ldb0283; OppDII, Ldb0284; and OppFII, Ldb0285) were also significantly up-regulated (> three-fold). Higher expression levels of above transporters strengthened the nutrient uptake, especial for glucose, amino acids, and peptides, which may be beneficial for biomass and D-LA synthesis.

Genetic information processing and nucleotide metabolism

Bacterial growth is directly correlated to the synthesis of protein and DNA. In this study, nine proteins related with aminoacyl-tRNA biosynthesis (i.e., phenylalanine–tRNA ligase beta subunit (PheT, Ldb1486), aspartyl-tRNA synthetase (AspS, Ldb0889), etc.) were observed with higher abundances under the N_2–PE–YE–$Ca(OH)_2$ condition compared with the control, indicating that aminoacyl-tRNA biosynthesis was activated. Moreover, elongation factor Ts (Tsf, Ldb1344) and more than ten ribosomal proteins, such as 50S ribosomal protein L5 (RplE, Ldb0408), and 30S ribosomal protein S1 (RpsA, Ldb0851), were also present at higher levels. Tsf mediates the regeneration of EF-Tu-GDP complex, which catalyzes the addition of aminoacyl-tRNA into ribosome [28]. Meanwhile, DNA topoisomerase 1 (TopA, Ldb1273), DNA-directed RNA polymerase subunit beta (RpoB, Ldb0386), DNA-directed RNA polymerase subunit beta'

(RpoC, Ldb0387), transcriptional regulator AsnC family (Ldb0493), and transcriptional regulator Crp family (Ldb0482), which were involved in the transcription and replication processes, were also up-regulated. Additionally, two cell division proteins (i.e., FtsZ and FtsA) were of higher abundances. FtsZ plays a central role in the course of cell division, and may participate in the reconstruction of cell wall [19]. FtsZ and FtsA proteins assemble into a ring at midcell and are dedicated to septal peptidoglycan synthesis [34]. The up-regulated FtsZ and FtsA might accelerate cell division and growth. Since the production of D-LA was growth-related, these proteins with higher expression levels could efficiently enhance the cell growth, leading to higher D-LA production under the N_2–PE–YE–$Ca(OH)_2$ condition as shown in Fig. 1.

Stress response

In general, protein quality control, including refolding or degradation of damaged proteins, plays an indispensable role for cell survival, and the synthesis of chaperones and proteases are quickly induced under stress conditions to combat with the potentially deleterious aggregation of denatured proteins [36]. In this study, two chaperone proteins, DnaK (Ldb1313) and DnaJ (Ldb1312) were significantly down-regulated under the N_2–PE–YE–$Ca(OH)_2$ condition. A chaperone system consisting of DnaK, DnaJ, and a nucleotide exchange factor (GrpE), can efficiently refold misfolded proteins [48]. In *L. lactis*, acid stress induced the expression of DnaK [10]. In regard to the protease system, three proteins of Clp family, i.e., ClpX (Ldb0778), ClpE (Ldb0574), and ClpP (Ldb0624), were also observed with lower abundances. The Clp machinery is probably the main system for general protein turnover in LAB [36]. For example, the ClpP of *L. lactis* plays a key role in hydrolysis of misfolded proteins and modulation of intracellular key regulatory protein level [43]. The lower expression of chaperones and proteases probably indicated the less intracellular protein misfolding, thereby fewer responses of protein repair. Besides, several proteins related with stress response, such as protease HtpX homolog (HtpX1, Ldb0160), thioredoxin (TrxA2, Ldb1524), response regulator of two-component system (Ldb0688), sensor histidine kinase of two-component system (Ldb0689), and universal stress protein (Usp, Ldb0718), were also down-regulated.

The down-regulation of stress-related proteins suggested that the cell growth was in a more suitable state, i.e., under a lower stress environment. Therefore, it did not have to induce superfluous stress response. The lower stress meant that the cells were suffered to less damage. The oxidative, acid, and osmotic stress will damage cell envelope, DNA and proteins [50]. To survive, cells will activate a series of related stress response, such as hydrolysis of denatured proteins, refolding of misfolded proteins, etc., to withstand the cell damage caused by stress. High stress not only causes cell damage, which affects the normal metabolism, but also induces the synthesis of a mass of repair proteins, which results in metabolic burden [36]. Therefore, in this study, lower stress would be beneficial for cell survival and growth.

Proposed metabolic mechanisms of D-LA overproduction by *L. delbrueckii* under the N_2–PE–YE–$Ca(OH)_2$ condition

Based on the results of metabolomic and proteomic analysis, the metabolic responses of *L. delbrueckii* to the combined fermentation condition (N_2–PE–YE–$Ca(OH)_2$) are summarized and described in Fig. 6.

On one hand, proteomic analysis showed that most proteins with higher abundances were involved in EMP pathway, PP pathway, amino acid metabolism, peptide hydrolysis, glucose-specific PTS, and amino acid and peptide transport. Thereby, the enhanced flux into central carbon metabolism and the sufficient cellular building blocks, ATP and reducing equivalents for maintaining the cell robustness significantly promoted the D-LA synthesis. In particular, the EMP pathway was greatly activated under the combined condition, which could supply more precursors for D-LA synthesis. Meanwhile, the improvement of transcription, translation, and cell division processes also helped to accelerate the protein synthesis and bacteria growth. As a growth-related product, the increased quantity of biomass would also improve D-LA production. Moreover, metabolomic analysis indicated that the combined condition exerted a great positive effect on central carbon metabolism and amino acid metabolism (Fig. 3).

On the other hand, the identified proteins with lower abundances were mainly involved in energy metabolism, stress response, and bypass of pyruvate. The decrease of expression levels in F_0F_1-ATPase subunits indicated that the higher pH under the combined condition would reduce the ATP cost for exporting protons by F_0F_1-ATPase, and more ATP could be consumed in the synthesis of building blocks and D-LA. In addition, the lower abundances of several chaperones, proteases and other stress response proteins suggested that the combined condition might reduce the protein misfolding and denaturation, and supply a better intracellular state for D-LA production. Consistently, the metabolomic analysis also identified several metabolites (trehalose and glutamate) related with stress response, present at lower relative abundances (Supplementary Materials B: Fig. S1). Moreover, the decreased flux from pyruvate to acetyl-CoA supplied more pyruvate for D-LA synthesis.

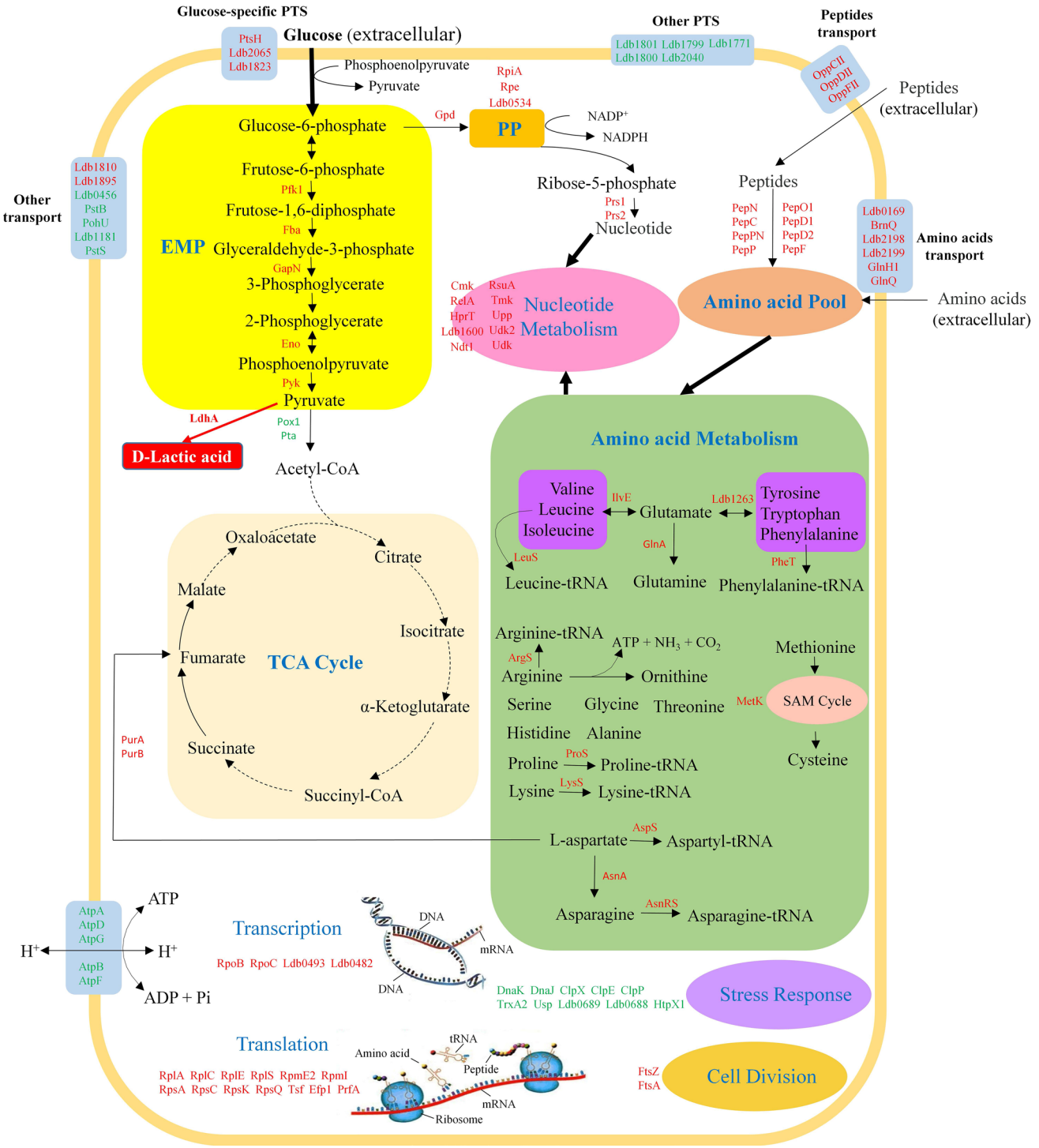

Fig. 6 Scheme of metabolic pathways in D-LA production by *L. delbrueckii* under N_2–PE–YE–$Ca(OH)_2$ condition. The up- and down-regulated proteins are presented as red and green fonts, respectively. The dotted arrows represent the TCA cycle might be incomplete. Regions of different colors represent different metabolic modules. The detailed information of each protein can be found in supplementary material (Supplementary Materials A: Table S2)

In summary, according to the cellular roles of differentially expressed proteins, intracellular metabolism was significantly changed under the N_2–PE–YE–$Ca(OH)_2$ condition, including central carbon metabolism, energy metabolism, amino acid metabolism, peptide hydrolysis, transport, genetic information processing, and stress

response. Further analysis of these metabolic pathways revealed that glycolysis and pentose phosphate pathways, transport of glucose, amino acids and peptides, amino acid metabolism, peptide hydrolysis, synthesis of nucleotides and proteins, and cell division were all strengthened, while ATP consumption for exporting proton, cell damage, metabolic burden caused by stress response, and bypass of pyruvate were decreased under the combined condition. These might be the main reasons for significantly improved D-LA production. These findings demonstrated that the D-LA synthesis was under a sophisticated and systematic regulation, although it was a simple in vivo reduction reaction.

Conclusion

In this work, various fermentation conditions were first identified and their effects on D-LA biosynthesis were further investigated in *L. delbrueckii* based on the systematic metabolomic and proteomic analysis. The final D-LA titer could reach to 133 g/L, 1.71-fold improvement under the optimally combined condition compared with the control. Metabolomic analysis showed that different fermentation conditions exerted different influences on changes of intracellular metabolism and phenotypes. Proteomic analysis revealed that intracellular metabolism has been significantly influenced under the combined fermentation condition, including central carbon metabolism, amino acid metabolism, peptide hydrolysis, transport, genetic information processing, and stress response. These findings will provide an important view for the further improvement of D-LA production in the future.

Acknowledgements This work was financially supported by the National Natural Science Foundation of China (no. 21676189); and the key technologies R & D program of Tianjin (no. 16YFZCSY00780).

References

1. Abdel-Banat BMA, Hoshida H, Ano A, Nonklang S, Akada R (2010) High-temperature fermentation: how can processes for ethanol production at high temperatures become superior to the traditional process using mesophilic yeast? Appl Microbiol Biotechnol 85:861–867. https://doi.org/10.1007/s00253-009-2248-5
2. Bai Z, Gao Z, Sun J, Wu B, He B (2016) D-Lactic acid production by *Sporolactobacillus inulinus* YBS1-5 with simultaneous utilization of cottonseed meal and corncob residue. Bioresour Technol 207:346–352. https://doi.org/10.1016/j.biortech.2016.02.007
3. Berry AR, Franco CMM, Zhang W, Middelberg APJ (1999) Growth and lactic acid production in batch culture of *Lactobacillus rhamnosus* in a defined medium. Biotechnol Lett 21:163–167. https://doi.org/10.1023/a:1005483609065
4. Christensen J, Dudley E, Pederson JA, Steele J (1999) Peptidases and amino acid catabolism in lactic acid bacteria. Antonie Van Leeuwenhoek 76(1–4):217–246. https://doi.org/10.1023/a:1002001919720
5. Courant F, Martzolff A, Rabin G, Antignac J-P, Le Bizec B, Giraudeau P, Tea I, Akoka S, Couzinet A, Cogne G, Grizeau D, Goncalves O (2013) How metabolomics can contribute to bioprocesses: a proof of concept study for biomarkers discovery in the context of nitrogen-starved microalgae grown in photobioreactors. Metabolomics 9:1286–1300. https://doi.org/10.1007/s11306-013-0532-y
6. Ding M-Z, Cheng J-S, Xiao W-H, Qiao B, Yuan Y-J (2009) Comparative metabolomic analysis on industrial continuous and batch ethanol fermentation processes by GC–TOF–MS. Metabolomics 5:229–238. https://doi.org/10.1007/s11306-008-0145-z
7. Fernández M, Zúñiga M (2006) Amino acid catabolic pathways of lactic acid bacteria. Crit Rev Microbiol 32:155–183. https://doi.org/10.1080/10408410600880643
8. Fodinger M, Horl WH, Sunder-Plassmann G (2000) Molecular biology of 5,10-methylenetetrahydrofolate reductase. J Nephrol 13:20–33
9. Francl AL, Thongaram T, Miller MJ (2010) The PTS transporters of *Lactobacillus gasseri* ATCC 33323. BMC Microbiol 10:77. https://doi.org/10.1186/1471-2180-10-77
10. Frees D, Vogensen FK, Ingmer H (2003) Identification of proteins induced at low pH in *Lactococcus lactis*. Int J Food Microbiol 87:293–300. https://doi.org/10.1016/s0168-1605(03)00104-1
11. Fu X, Wang Y, Wang J, Garza E, Manow R, Zhou S (2017) Semi-industrial scale (30 m^3) fed-batch fermentation for the production of D-lactate by *Escherichia coli* strain HBUT-D15. J Ind Microbiol Biotechnol 44:221–228. https://doi.org/10.1007/s10295-016-1877-9
12. Fukushima K, Chang Y-H, Kimura Y (2007) Enhanced stereocomplex formation of poly(L-lactic acid) and poly(D-lactic acid) in the presence of stereoblock poly(lactic acid). Macromol Biosci 7:829–835. https://doi.org/10.1002/mabi.200700028
13. Gan CS, Chong PK, Pham TK, Wright PC (2007) Technical, experimental, and biological variations in isobaric tags for relative and absolute quantitation (iTRAQ). J Proteome Res 6:821–827. https://doi.org/10.1021/pr060474i
14. Gao X, Sun T, Wu L, Chen L, Zhang W (2017) Co-overexpression of response regulator genes slr1037 and sll0039 improves tolerance of *Synechocystis* sp PCC 6803 to 1-butanol. Bioresour Technol 245:1476–1483. https://doi.org/10.1016/j.biortech.2017.04.112
15. Garlotta D (2001) A literature review of poly(lactic acid). J Polym Environ 9:63–84. https://doi.org/10.1023/a:1020200822435
16. Giraud E, Lelong B, Raimbault M (1991) Influence of pH and initial lactate concentration on the growth of *Lactobacillus plantarum*. Appl Microbiol Biotechnol 36:96–99. https://doi.org/10.1007/bf00164706
17. Glaasker E, Heuberger EHML, Konings WN, Poolman B (1998) Mechanism of osmotic activation of the quaternary ammonium compound transporter (QacT) of *Lactobacillus plantarum*. J Bacteriol 180:5540
18. Glaasker E, Konings WN, Poolman B (1996) Osmotic regulation of intracellular solute pools in *Lactobacillus plantarum*. J Bacteriol 178:575
19. Goehring NW, Beckwith J (2005) Diverse paths to midcell: assembly of the bacterial cell division machinery. Curr Biol 15:R514–R526. https://doi.org/10.1016/j.cub.2005.06.038
20. Guerzoni ME, Lanciotti R, Cocconcelli PS (2001) Alteration in cellular fatty acid composition as a response to salt, acid, oxidative and thermal stresses in *Lactobacillus helveticus*. Microbiology 147:2255–2264. https://doi.org/10.1099/00221287-147-8-2255
21. Hofvendahl K, Hahn-Hagerdal B (2000) Factors affecting the fermentative lactic acid production from renewable resources.

Enzyme Microb Technol 26:87–107. https://doi.org/10.1016/s0141-0229(99)00155-6
22. Hua Y, Wang S, Liu Z, Liu X, Zou L, Gu W, Hou Y, Ma Y, Luo Y, Liu J (2016) iTRAQ-based quantitative proteomic analysis of cultivated *Pseudostellaria heterophylla* and its wild-type. J Proteom 139:13–25. https://doi.org/10.1016/j.jprot.2016.02.027
23. Hutkins RW, Nannen NL (1993) pH homeostasis in lactic acid bacteria. J Dairy Sci 76:2354–2365. https://doi.org/10.3168/jds.S0022-0302(93)77573-6
24. Klotz S, Kaufmann N, Kuenz A, Prüße U (2016) Biotechnological production of enantiomerically pure D-lactic acid. Appl Microbiol Biotechnol 100:9423–9437. https://doi.org/10.1007/s00253-016-7843-7
25. Klotz S, Kuenz A, Pruesse U (2017) Nutritional requirements and the impact of yeast extract on the D-lactic acid production by *Sporolactobacillus inulinus*. Green Chem 19:4633–4641. https://doi.org/10.1039/c7gc01796k
26. Koponen J, Laakso K, Koskenniemi K, Kankainen M, Savijoki K, Nyman TA, de Vos WM, Tynkkynen S, Kalkkinen N, Varmanen P (2012) Effect of acid stress on protein expression and phosphorylation in *Lactobacillus rhamnosus* GG. J Proteom 75:1357–1374. https://doi.org/10.1016/j.jprot.2011.11.009
27. Li J, Sun J, Wu B, He B (2017) Combined utilization of nutrients and sugar derived from wheat bran for D-lactate fermentation by *Sporolactobacillus inulinus* YBS1-5. Bioresour Technol 229:33–38. https://doi.org/10.1016/j.biortech.2016.12.101
28. Liu H, Huang D, Jin L, Wang C, Liang S, Wen J (2017) Integrating multi-omics analyses of *Nonomuraea dietziae* to reveal the role of soybean oil in [(4′-OH)MeLeu]4-CsA overproduction. Microb Cell Fact 16:120. https://doi.org/10.1186/s12934-017-0739-0
29. Lv L-X, Yan R, Shi H-Y, Shi D, Fang D-Q, Jiang H-Y, Wu W-R, Guo F-F, Jiang X-W, Gu S-L, Chen Y-B, Yao J, Li L-J (2017) Integrated transcriptomic and proteomic analysis of the bile stress response in probiotic *Lactobacillus salivarius* LI01. J Proteom 150:216–229. https://doi.org/10.1016/j.jprot.2016.08.021
30. Marty-Teysset C, de la Torre F, Garel JR (2000) Increased production of hydrogen peroxide by *Lactobacillus delbrueckii* subsp bulgaricus upon aeration: involvement of an NADH oxidase in oxidative stress. Appl Environ Microbiol 66:262–267. https://doi.org/10.1128/aem.66.1.262-267.2000
31. Mimitsuka T, Na K, Morita K, Sawai H, Minegishi S, Henmi M, Yamada K, Shimizu S, Yonehara T (2012) A membrane-integrated fermentation reactor system: its effects in reducing the amount of sub-raw materials for D-lactic acid continuous fermentation by *Sporolactobacillus laevolacticus*. Biosci Biotechnol Biochem 76:67–72. https://doi.org/10.1271/bbb.110499
32. Miyoshi A, Rochat T, Gratadoux J-J, Le Loir Y, Oliveira SC, Langella P, Azevedo V (2003) Oxidative stress in *Lactococcus lactis*. Genet Mol Res 2:348–359
33. Morishita T, Yajima M (1995) Incomplete operation of biosynthetic and bioenergetic functions of the citric acid cycle in multiple auxotrophic *Lactobacilli*. Biosci Biotechnol Biochem 59:251–255. https://doi.org/10.1271/bbb.59.251
34. Mura A, Fadda D, Perez AJ, Danforth ML, Musu D, Rico AI, Krupka M, Denapaite D, Tsui H-CT, Winkler ME, Branny P, Vicente M, Margolin W, Massidda O (2017) Roles of the essential protein FtsA in cell growth and division in *Streptococcus pneumoniae*. J Bacteriol. https://doi.org/10.1128/jb.00608-16
35. Nakano S, Ugwu CU, Tokiwa Y (2012) Efficient production of D-(−)-lactic acid from broken rice by *Lactobacillus delbrueckii* using $Ca(OH)_2$ as a neutralizing agent. Bioresour Technol 104:791–794. https://doi.org/10.1016/j.biortech.2011.10.017
36. Papadimitriou K, Alegria A, Bron PA, de Angelis M, Gobbetti M, Kleerebezem M, Lemos JA, Linares DM, Ross P, Stanton C, Turroni F, van Sinderen D, Varmanen P, Ventura M, Zuniga M, Tsakalidou E, Kok J (2016) Stress physiology of lactic acid bacteria. Microbiol Mol Biol Rev 80:837–890. https://doi.org/10.1128/mmbr.00076-15
37. Papagianni M, Avramidis N (2011) *Lactococcus lactis* as a cell factory: a twofold increase in phosphofructokinase activity results in a proportional increase in specific rates of glucose uptake and lactate formation. Enzyme Microb Technol 49:197–202. https://doi.org/10.1016/j.enzmictec.2011.05.002
38. Papagianni M, Avramidis N, Filiousis G (2007) Glycolysis and the regulation of glucose transport in *Lactococcus lactis* spp. lactis in batch and fed-batch culture. Microb Cell Fact 6:16. https://doi.org/10.1186/1475-2859-6-16
39. Partanen L, Marttinen N, Alatossava T (2001) Fats and fatty acids as growth factors for *Lactobacillus delbrueckii*. Syst Appl Microbiol 24:500–506. https://doi.org/10.1078/0723-2020-00078
40. Pei G, Chen L, Zhang W (2017) Chapter nine-WGCNA application to proteomic and metabolomic data analysis. Methods Enzymol 585:135–158
41. Purvis JE, Yomano LP, Ingram LO (2005) Enhanced trehalose production improves growth of *Escherichia coli* under osmotic stress. Appl Environ Microbiol 71:3761–3769. https://doi.org/10.1128/aem.71.7.3761-3769.2005
42. Roudot-Algaron F, Yvon M (1998) Aromatic and branched chain amino acids catabolism in *Lactococcus lactis*. Lait 78:23–30
43. Savijoki K, Ingmer H, Varmanen P (2006) Proteolytic systems of lactic acid bacteria. Appl Microbiol Biotechnol 71:394–406
44. Serrazanetti DI, Ndagijimana M, Sado-Kamdem SL, Corsetti A, Vogel RF, Ehrmann M, Guerzoni ME (2011) Acid stress-mediated metabolic shift in *Lactobacillus sanfranciscensis* LSCE1. Appl Environ Microbiol 77:2656–2666. https://doi.org/10.1128/AEM.01826-10
45. Su Y, Wang J, Shi M, Niu X, Yu X, Gao L, Zhang X, Chen L, Zhang W (2014) Metabolomic and network analysis of astaxanthin-producing *Haematococcus pluvialis* under various stress conditions. Bioresour Technol 170:522–529. https://doi.org/10.1016/j.biortech.2014.08.018
46. Sun J, Wang Y, Wu B, Bai Z, He B (2015) Enhanced production of D-lactic acid by *Sporolactobacillus* sp Y2-8 mutant generated by atmospheric and room temperature plasma. Biotechnol Appl Biochem 62:287–292. https://doi.org/10.1002/bab.1267
47. Tokiwa Y, Calabia BP (2006) Biodegradability and biodegradation of poly(lactide). Appl Microbiol Biotechnol 72:244–251. https://doi.org/10.1007/s00253-006-0488-1
48. Turgay K (2011) Role of proteolysis and chaperones in stress response and regulation. Bacterial stress responses, 2nd edn. American Society of Microbiology, Washington, DC, pp 75–90
49. van de Guchte M, Penaud S, Grimaldi C, Barbe V, Bryson K, Nicolas P, Robert C, Oztas S, Mangenot S, Couloux A, Loux V, Dervyn R, Bossy R, Bolotin A, Batto JM, Walunas T, Gibrat JF, Bessieres P, Weissenbach J, Ehrlich SD, Maguin E (2006) The complete genome sequence of *Lactobacillus bulgaricus* reveals extensive and ongoing reductive evolution. Proc Natl Acad Sci USA 103:9274–9279. https://doi.org/10.1073/pnas.0603024103
50. van de Guchte M, Serror P, Chervaux C, Smokvina T, Ehrlich SD, Maguin E (2002) Stress responses in lactic acid bacteria. Antonie Van Leeuwenhoek Int J Gen Mol Microbiol 82:187–216. https://doi.org/10.1023/a:1020631532202
51. Wang C, Liu J, Liu H, Liang S, Wen J (2017) Combining metabolomics and network analysis to improve tacrolimus production in *Streptomyces tsukubaensis* using different exogenous feedings. J Ind Microbiol Biotechnol 44:1527–1540. https://doi.org/10.1007/s10295-017-1974-4
52. Wang G, Huang D, Qi H, Wen J, Jia X, Chen Y (2013) Rational medium optimization based on comparative metabolic profiling

analysis to improve fumaric acid production. Bioresour Technol 137:1–8. https://doi.org/10.1016/j.biortech.2013.03.041
53. Wang J, Hui W, Cao C, Jin R, Ren C, Zhang H, Zhang W (2016) Proteomic analysis of an engineered isolate of *Lactobacillus plantarum* with enhanced raffinose metabolic capacity. Sci Rep 6:31403. https://doi.org/10.1038/srep31403
54. Wang L, Zhao B, Li F, Xu K, Ma C, Tao F, Li Q, Xu P (2011) Highly efficient production of D-lactate by *Sporolactobacillus* sp. CASD with simultaneous enzymatic hydrolysis of peanut meal. Appl Microbiol Biotechnol 89:1009–1017. https://doi.org/10.1007/s00253-010-2904-9
55. Xia M, Huang D, Li S, Wen J, Jia X, Chen Y (2013) Enhanced FK506 production in *Streptomyces tsukubaensis* by rational feeding strategies based on comparative metabolic profiling analysis. Biotechnol Bioeng 110:2717–2730. https://doi.org/10.1002/bit.24941
56. Yu X, Niu X, Zhang X, Pei G, Liu J, Chen L, Zhang W (2015) Identification and mechanism analysis of chemical modulators enhancing astaxanthin accumulation in *Haematococcus pluvialis*. Algal Res 11:284–293. https://doi.org/10.1016/j.algal.2015.07.006
57. Zhai Z, Douillard FP, An H, Wang G, Guo X, Luo Y, Hao Y (2014) Proteomic characterization of the acid tolerance response in *Lactobacillus delbrueckii* subsp bulgaricus CAUH1 and functional identification of a novel acid stress-related transcriptional regulator Ldb0677. Environ Microbiol 16:1524–1537. https://doi.org/10.1111/1462-2920.12280
58. Zhang B, Horvath S (2005) A general framework for weighted gene co-expression network analysis. Stat Appl Genet Mol Biol 4:Article 17
59. Zhao J, Baba T, Mori H, Shimizu K (2004) Effect of *zwf* gene knockout on the metabolism of *Escherichia coli* grown on glucose or acetate. Metab Eng 6:164–174. https://doi.org/10.1016/j.ymben.2004.02.004